PHYSICAL REVIEW B VOLUME 19, NUMBER 1 1 JANUARY 1979

Spectroscopic study of the field-induced spin reorientation in $ErCrO_3$

K. Toyokawa*
Department of Physics, Faculty of Science, Osaka University, Toyonaka, Osaka 560, Japan

S. Kurita
Faculty of Engineering, Yokohama National University, Yokohama 240, Japan

K. Tsushima
Broadcasting Science Research Laboratories of Nippon Hōsō Kyōkai (Japan Broadcasting Corporation), Setagaya-ku, Tokyo 157, Japan

(Received 4 April 1978)

Using the optical Zeeman absorption spectrum of Er^{3+} and Cr^{3+} in $ErCrO_3$, the field-induced spin reorientations between Γ_1, Γ_2, and Γ_4 phases are investigated extensively. The data are analyzed using a two-sublattice molecular-field model. It is concluded that not only the antisymmetric exchange interactions between Cr^{3+} and Er^{3+} ions, but also the anisotropic symmetric ones are responsible for the spin reorientation. Comparing the ground-doublet splitting of the Er^{3+} ion between the Γ_1, Γ_4, and Γ_2 phases, the anisotropic symmetric part is separable from the predominant antisymmetric part. The anisotropic-symmetric to the antisymmetric-part rate is about 0.33.

I. INTRODUCTION

The magneto-optical properties of rare-earth orthochromites $RCrO_3$, where R can be yttrium or a rare-earth, have been extensively investigated in recent years. Aoyagi *et al.*[1] first reported direct observation of Davydov-split exciton lines associated with the Cr^{3+} R excitation on $YCrO_3$. Later, Davydov splittings have been observed by Meltzer[2] in the absorption lines of $ErCrO_3$, and $HoCrO_3$.

On the other hand, it is well known that the $RCrO_3$, as well as the rare-earth orthoferrites $RFeO_3$, show interesting magnetic properties such as spin reorientation (SR) induced by the temperature and magnetic field.

In $RCrO_3$, there are three types of magnetic interaction, Cr^{3+}-Cr^{3+}, Cr^{3+}-R^{3+}, and R^{3+}-R^{3+}, each of which generally consists of the isotropic, the anisotropic antisymmetric, and symmetric superexchange interactions. Yamaguchi *et al.*[3,4] have shown that the anisotropic parts of the magnetic interactions between Cr^{3+} and R^{3+} are generally responsible for SR.

Optical spectroscopy is one of the most powerful methods to study the SR of $RCrO_3$ microscopically. One of the reasons is that the magnetic-symmetry change associated with SR is directly reflected in the selection rules of the polarized absorption spectra.[2,5] The other reason is that the parameters of the magnetic interactions can be directly estimated through the analysis of the observed spectra of Cr^{3+} and R^{3+}, especially R^{3+}. As the optical spectra of R^{3+} are generally sharp, the effect of magnetic interactions between Cr^{3+} and R^{3+}, and R^{3+} and R^{3+}, is reflected sensitively in the spectra. $ErCrO_3$ is one of the suitable materials for the spectroscopic study.

There have been several quantitative studies of the SR of $ErCrO_3$.[6,7] These studies, however, are not completely satisfactory from both the experimental and the analytical viewpoint since the magnetic phase diagram of $ErCrO_3$ is not determined completely owing to the lack of measurements for the Γ_2 phase, and the anisotropic parts of the magnetic interactions between Cr^{3+} and R^{3+} are not fully taken into account in the analysis.

The purpose of the present paper is to report a detailed spectroscopic study of the SR, enough to determine the magnetic phase diagram, and a more reasonable analysis by taking into consideration all the magnetic interactions between Cr^{3+} and Er^{3+}, allowed by the symmetry.

$ErCrO_3$ has been studied by neutron-diffraction,[8,9] bulk-magnetization, and susceptibility measurements,[9-11] specific-heat,[9,12] Mössbauer measurements,[13] and optical-absorption spectroscopy of Cr^{3+} and Er^{3+} energy levels.[6,7,14]

We briefly summarize the important properties. The crystal has an orthorhombically distorted perovskite structure (space group D_{2h}^{16}-$Pbnm$) with four molecules per unit cell. The point symmetry of the Er^{3+} site is C_{1h}. The chromium ions below $T_{N1}=133$ K order antiferromagnetically with a weak ferromagnetic moment, in Bertaut's notation[15,16] $\Gamma_4(G_x, A_y, F_z; F_z^R)$. In Fig. 1, the various spin configurations of $ErCrO_3$ are shown. At $T_{Sr}=9.3$ K, $ErCrO_3$ undergoes a spin reorientation from Γ_4 to $\Gamma_1(A_x, G_y, C_z; C_z^R)$ where the weak ferromagnetic moment disappears. The transition is

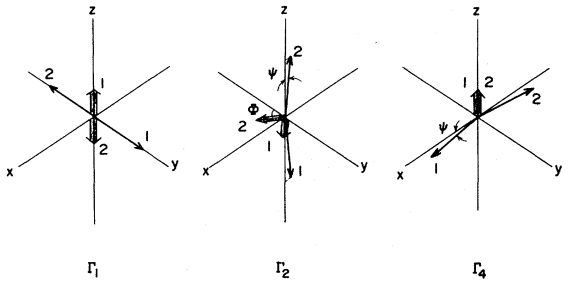

FIG. 1. Spin arrangements of orthochromites in the two-sublattice approximation. The long arrows labeled 1, 2 denote chromium, and the shorter ones (also 1,2) rare earths. ψ and Φ are canting angles of the chromium and rare-earth spins, respectively.

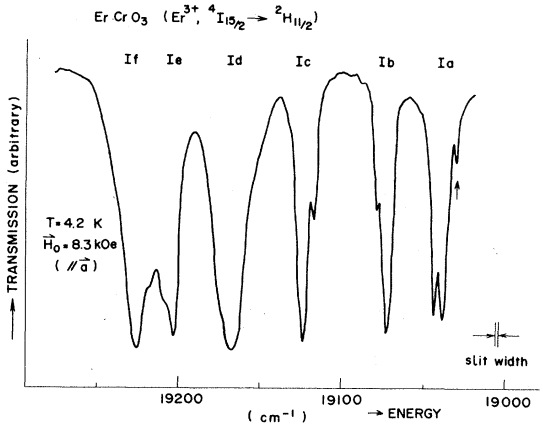

FIG. 2. Optical-absorption spectra of Er^{3+} in $ErCrO_3$ for $\vec{E} \parallel \vec{a}$ with $\vec{H}_0 \parallel \vec{a}$. I refers to the lowest Kramers doublet of the $^4I_{15/2}$, and a, b, c, d, e, and f to the Kramers doublets of the $^2H_{11/2}$. The arrow at one of the I-a lines shows the transition from the upper-ground doublet of I to one of the excited doublets of a.

of first order. Below T_{Sr} the Γ_4 phase can be recovered by applying a small external field along the c axis.

The third spin configuration $\Gamma_2(F_x, C_y, G_z; F_x^R, C_y^R)$ can be induced in $ErCrO_3$ by an external field along the a axis. Above T_{Sr}, the field-induced SR has been observed from Γ_4 to Γ_2 by magnetization measurements[6,11] and by optical measurements.[6,14] There is an inconsistency, however, between the magnetization results[6] and the SR optical measurements[14] from Γ_1 to Γ_2 below T_{Sr}. The former result is that SR was observed with a magnetic field of 28 kOe along the a axis at 4.2 K. On the other hand, the latter result is that no SR was observed up to 43 kOe. In this paper, we describe an extensive optical study of the field-induced SR among Γ_2, Γ_1, and Γ_4 phases.

Following the experimental results in Sec. II, a two-sublattice molecular-field model is described in Sec. III A. By using this model, the field-induced SR's from Γ_1 to Γ_4 and from Γ_1 to Γ_2 are analyzed in Sec. III B and III C. The importance of the anisotropic symmetric exchange term between Cr^{3+} and Er^{3+} is emphasized as well as that of the antisymmetric one. In Sec. IV we summarize the results.

II. MEASUREMENTS AND RESULTS

A. Experimental

Single crystals of $ErCrO_3$ were grown by the flux method, using PbO and PbF as the flux. The crystallographic axes were determined by the Laue method. Flux free crystals were cut and polished to platelets having (001) and (110) faces, whose thicknesses were about 30 to 300 μm.

For the spectroscopic study a Nippon Bunko 1-m grating spectrometer and a Spex 1800 $\frac{3}{4}$-m grating spectrometer were used with a HTV R-636 photomultiplier. Photoelectric signals were amplified and converted into logarithmic scale by a home-made log amplifier, and recorded with a strip chart recorder.

A 20-kOe electromagnet and a 150-kOe superconducting magnet were used to obtain the magnetic field dependence of the spectrum. For the measurements below 4.2 K, the sample was immersed in liquid helium and for the measurements above 4.2 K, the sample was mounted in a variable-temperature Dewar in which the sample was surrounded by helium-exchange gas. The temperature of the sample was monitored by a Ge thermometer and a carbon resistor mounted near the sample. The fluctuations of the temperature during the measurements were negligible.

The absolute wave number was calibrated using a low-pressure mercury and neon light source.

B. Field-induced SR from Γ_1 to Γ_2

Figure 2 shows typical absorption spectra corresponding to $^4I_{15/2}$-$H_{11/2}$ transitions of Er^{3+} ions with the field parallel to the a axis. Below liquid-helium temperature, only the transitions from the lowest Kramers doublet of the $^4I_{15/2}$ ground state I to the six Kramers doublets of $^2H_{11/2}$ labeled as a, b, c, d, e, and f in order of increasing energy, can be observed.

Figure 3 shows the Zeeman spectra of the I-a and I-b transitions. The spectra shift linearly as a function of the external magnetic field H_0 except at $H_0 = H_c$. At $H_0 = H_c$, no discontinuity is seen within experimental resolution, but the spectroscopic splitting factors, in other words, the effec-

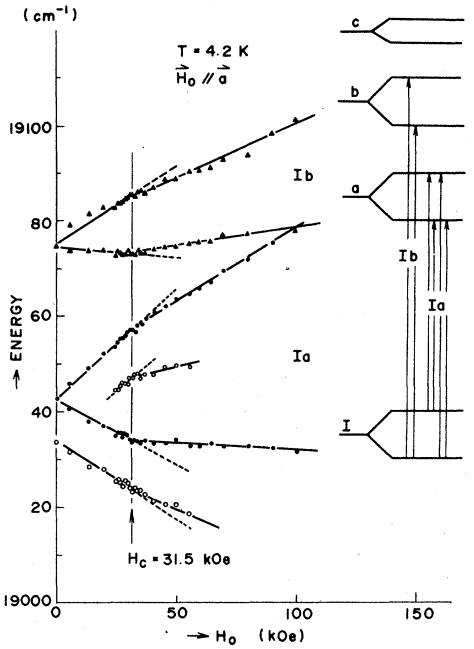

FIG. 3. Optical-absorption spectra of Er^{3+} in $ErCrO_3$ with $\vec{H}_0 \| \vec{a}$. In the *I-b* transition, the spectra from the upper ground doublet to the excited *b* doublet are hidden in the linewidth. The field dependences of the *I-c*, *I-d*, *I-e*, and *I-f* transitions are similar, and are not shown.

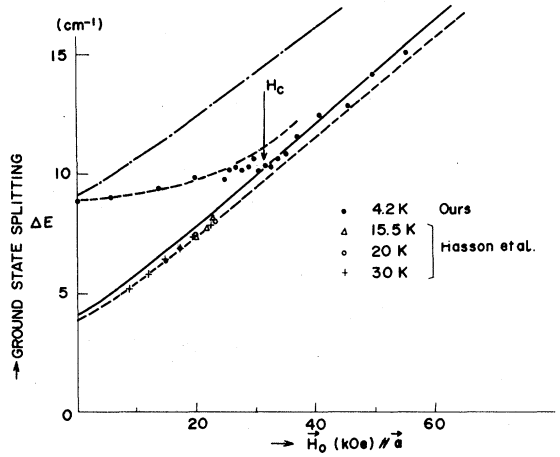

FIG. 4. Observed ground-state splitting, ΔE, of Er^{3+} ions with $\vec{H}_0 \| \vec{a}$. The black circles are our data, and the other data are by Hasson *et al.* (Ref. 14). The solid, dashed, and the dotted curves are the best-fit results of the calculations. The dash-dotted curve is the result without taking into account the $\tilde{a}$ term. For details, see text.

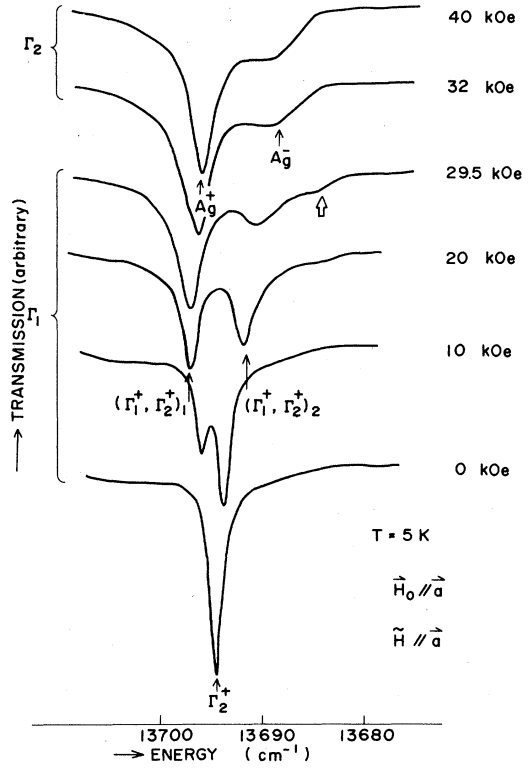

FIG. 5. Magnetic field dependence of the Cr^{3+} exciton spectra in $ErCrO_3$ for $\vec{H} \| \tilde{a}$ with $\vec{H}_0 \| \vec{a}$. The critical field is 30 kOe at $T = 5$ K. (Γ_1^+, Γ_2^+) in Ref. 5 is the notation for the exciton states in the Γ_1 phase under a magnetic field, while A_g^+ and A_g^- are the notation for the Γ_2 phase.

tive *g* values of these levels change. From the *I-a* transition, the ground doublet splitting ΔE of Er^{3+} can be observed directly, which is an important parameter to estimate the magnetic interactions in $ErCrO_3$. Figure 4 shows the observed ΔE as a function of H_0 along the *a* axis. Also shown are the results in the Γ_2 phase at higher temperature.[6]

Except at H_c, no anomaly of optical spectra of Er^{3+} is observed with fields up to 150 kOe. We assume that the field-induced SR from Γ_1 to Γ_2 occurs at $H_0 = H_c$. To confirm this, we observed the well established Cr^{3+} exciton lines as a function of H_0 along the *a* axis, which are illustrated in Fig. 5.

Comparing the polarized spectral data of the Cr^{3+} exciton between Γ_1, Γ_2, and Γ_4 states of several $RCrO_3$,[2] and by theoretical analysis considering magnetic symmetry under applied magnetic field, it is concluded that the field-induced SR from Γ_1 to Γ_2 occurs in the regions of $H_0 = H_c$. Two extra weak absorption lines, one of which is shown by a white arrow in Fig. 5, are observed near, but below H_c. These lines are not identified and remain to be explained.

Figure 6 shows the experimental results of the temperature dependence of the reorientation field from Γ_1 to Γ_2. Also shown are the results of the

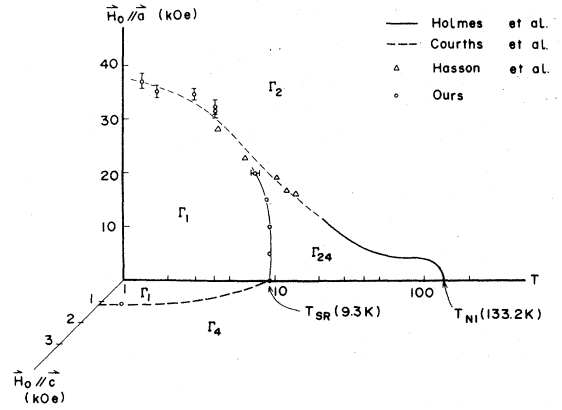

FIG. 6. Magnetic phase diagram of $ErCrO_3$ as function of temperature and external magnetic field along the a and c axes. Also shown are published data by other authors (Refs. 6, 11, and 14).

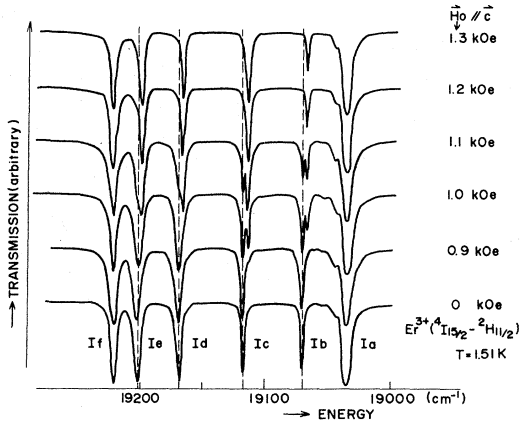

FIG. 7. Optical spectra of the $^4I_{15/2}$-$^2H_{11/2}$ transitions of Er^{3+} in $ErCrO_3$ with $\vec{H}_0 \| \vec{c}$ and $\vec{E}_0 \| \vec{c}$. The notations I and a-f refer to Kramers doublets of $^4I_{15/2}$ and of $^2H_{11/2}$, respectively. No demagnetization correction is made.

other authors.[6,11,14] Our results are slightly higher than that of Hassons. The extrapolated value of the reorientation field H_c to 0 K is about 37 kOe.

C. Field- and temperature-induced SR from Γ_1 to Γ_4

We observed the field-induced SR from Γ_1 to Γ_4 under the magnetic field H_0 along the c axis. Figure 7 shows the field dependence of the optical spectra for the $^4I_{15/2}$ - $^2H_{11/2}$ transition. As is clearly shown, several lines split into two lines near $H_0 = 1$ kOe. This effect is considered to come from the coexistence of two phases, Γ_1 and Γ_4, due to the demagnetization field when the external magnetic field approaches the reorientation field. In the Γ_1 phase, the induced net magnetization is small under applied magnetic field and the demagnetization field is negligible. Our result for the reorientation field from Γ_1 to Γ_4 is 1.0 kOe at 1.51 K.

We also observed the temperature-induced SR from Γ_1 to Γ_4 with H_0 parallel to the a axis. When H_0 is zero, the observed transition temperature T_{Sr} from Γ_1 to Γ_4 is 9.3 ± 0.2 K and this is consistent with the Courths result.[14] In the Γ_4 phase, it is well established that Cr^{3+} and Er^{3+} spins rotate continuously and the net moment rotates continuously in the a-c plane when the magnetic field is applied from zero along the a axis. The magnetic symmetry in this case is not Γ_4, but Γ_{24} with $\vec{H}_0 \| \vec{a}$.[4] Therefore, strictly speaking, we observed the temperature-induced SR from Γ_1 to Γ_{24}. The magnetic phase diagram of $ErCrO_3$ deduced from the optical observation is shown in Fig. 6, as a function of temperature and magnetic fields along the a and c axes. The observations of the crossing point of the two phase boundaries, Γ_1 - Γ_2 and Γ_1 - Γ_{24} were not carried out because of the need of higher resolution.

III. ANALYSIS

A. Model and general formalism

The Hamiltonian of our system is given as follows:

$$\mathcal{H} = \mathcal{H}^{Cr} + \mathcal{H}^{Cr\text{-}Er} + \mathcal{H}^{Er}, \tag{1}$$

where the first term represents the Hamiltonian for Cr^{3+} ions, the second that for the interactions between Cr^{3+} and rare-earth ions, and the third for rare-earth ions.

Yamaguchi[3] discussed the most general expression for the Hamiltonians of orthochromites and orthoferrites using group theoretical consideration, and gave the explicit form of the first and the second terms of Eq. (1), using the four sublattice approximation. The theory dealt with SR in which the $\mathcal{H}^{Cr\text{-}Er}$ term is most important, so that the contribution of $\mathcal{H}^{Er}$ was neglected.

On the other hand, we treat the field-induced SR at lower temperature than T_{Sr}, and cannot entirely neglect the third term $\mathcal{H}^{Er}$. In the following, the explicit mathematical form is written down in the two sublattice approximation, because the essential results do not differ from that of the four sublattice one. This makes the following discussions more transparent.

The Hamiltonian of the interaction of Cr^{3+} spins is

$$\mathcal{H}^{Cr} = J\vec{S}_1 \cdot \vec{S}_2 + D_y(S_{1x}S_{2z} - S_{1z}S_{2x}) - \tfrac{1}{2}K(S_{1x}^2 + S_{2x}^2) - \tfrac{1}{2}g\mu_B(\vec{S}_1 + \vec{S}_2)\cdot\vec{H}_0. \tag{2}$$

$\vec{S}_1$ and $\vec{S}_2$ represent the average spins of Cr^{3+} sublattices one and two, respectively. The first and the second terms are the isotropic and the antisymmetric exchange, respectively, the third term represents the single ion anisotropy, and the last the Zeeman interaction. The g value of the Cr^{3+} ion is regarded as isotropic.

The term $\mathcal{H}^{Cr-Er}$ consists of the isotropic, the anisotropic-antisymmetric and symmetric-exchange interactions between Cr^{3+} and Er^{3+} ions

$$\mathcal{H}^{Er-Cr} = \tfrac{1}{2}\tilde{J}(\vec{S}_1+\vec{S}_2)\cdot(\vec{\tilde{S}}_1+\vec{\tilde{S}}_2) - \tfrac{1}{2}\sum_{i,k=1,2}\vec{\tilde{D}}_{ik}\cdot(\vec{\tilde{S}}_i\times\vec{\tilde{S}}_k) + \tfrac{1}{2}\sum_{i,k=1,2}\vec{S}_i\cdot\vec{\tilde{a}}_{ik}\cdot\vec{\tilde{S}}_k , \quad (3)$$

where $\vec{S}_1$ and $\vec{S}_2$ are the average spins of Er^{3+} sublattices 1 and 2, respectively. In our model, Er^{3+} is treated as a fictitious spin, with $\tilde{S}=\frac{1}{2}$. The vector components of $\vec{\tilde{D}}_{ik}$ and the tensor components of $\vec{\tilde{a}}_{ik}$ in our approximation can be easily obtained from Yamaguchi's result [see Table I(e), I(f) in Ref. 3]. The previous works[6,14] did not take into account the anisotropic-symmetric interactions, the third term in Eq. (3). However, it will be shown to be important for the analysis of the SR in $ErCrO_3$. Our results are given in Tables I(a) and I(b).

The third term $\mathcal{H}^{Er}$ is given as follows:

$$\mathcal{H}^{Er} = \vec{\tilde{S}}_1\cdot J_1'\cdot\vec{\tilde{S}}_2 + \tfrac{1}{2}\sum_{k=1,2}\vec{\tilde{S}}_k\cdot\tilde{J}'_{2k}\cdot\vec{\tilde{S}}_k - \vec{D}'\cdot(\vec{\tilde{S}}_1\times\vec{\tilde{S}}_2) - \tfrac{1}{2}\mu_B\vec{H}_0(\vec{g}_1'\cdot\vec{\tilde{S}}_1+\vec{g}_2'\cdot\vec{\tilde{S}}_2), \quad (4)$$

where the terms represent first the sum of the isotropic exchange and the anisotropic-symmetric exchange between the 1 and 2 sublattices of Er^{3+}, second the sum of the isotropic exchange, the anisotropic-symmetric exchange within a sublattice and the anisotropy energy, third the antisymmetric exchange and fourth the Zeeman interactions. $\vec{g}_1'$ and $\vec{g}_2'$ are $\vec{g}$-tensors of Er^{3+} in sublattices 1 and 2, respectively.

The components of $\vec{J}_1'$, $\vec{J}_2'$, $\vec{D}$, $\vec{g}_1'$, and $\vec{g}_2'$ can be derived from the magnetic symmetry and are shown in Tables II(a), II(b), and II(c).

The free energy of the system described by Eq. (1) is defined as

$$F = \langle\mathcal{H}\rangle - T\sigma , \quad (5)$$

where $\langle\mathcal{H}\rangle$ is the thermal average of the Hamiltonian, T is temperature, and σ is the magnetic entropy of the system.

To calculate the free energy, we use the molecular field approximation and replace the mean value of the products of spin operators such as $\langle\vec{\tilde{S}}_i\cdot\vec{\tilde{S}}_j\rangle$ by the product of each mean value $\langle\vec{\tilde{S}}_i\rangle\langle\vec{\tilde{S}}_j\rangle$. Furthermore, the classical spin approximation is adopted. The detailed treatments are given in Refs. 4 and 6. Below we show only the important formula for analysis of the data.

By minimizing the free energy with respect to

TABLE I. (a) Antisymmetric-exchange-interaction constants between Cr and Er spins. (b) Anisotropic-symmetric-exchange-interaction constants between Cr and Er spins.

(a)

	$\vec{\tilde{S}}_1$	$\vec{\tilde{S}}_2$
$\vec{S}_1$	$(\tilde{D}_x, \tilde{D}_y, \tilde{D}_z)$	$(-\tilde{D}_x, \tilde{D}_y, -\tilde{D}_z)$
$\vec{S}_2$	$(-\tilde{D}_x, -\tilde{D}_y, \tilde{D}_z)$	$(\tilde{D}_x, -\tilde{D}_y, -\tilde{D}_z)$

(b)

$\vec{S}_1$	$\begin{pmatrix}\tilde{a}_{xx} & \tilde{a}_{xy} & \tilde{a}_{zx}\\ & \tilde{a}_{yy} & \tilde{a}_{yz}\\ & & \tilde{a}_{zz}\end{pmatrix}$	$\begin{pmatrix}\tilde{a}_{xx} & -\tilde{a}_{xy} & \tilde{a}_{zx}\\ & \tilde{a}_{yy} & -\tilde{a}_{yz}\\ & & \tilde{a}_{zz}\end{pmatrix}$
$\vec{S}_2$	$\begin{pmatrix}\tilde{a}_{xx} & \tilde{a}_{xy} & -\tilde{a}_{zx}\\ & \tilde{a}_{yy} & -\tilde{a}_{yz}\\ & & \tilde{a}_{zz}\end{pmatrix}$	$\begin{pmatrix}\tilde{a}_{xx} & -\tilde{a}_{xy} & -\tilde{a}_{zx}\\ & \tilde{a}_{yy} & \tilde{a}_{yz}\\ & & \tilde{a}_{zz}\end{pmatrix}$

TABLE II. (a) The components of the coupling tensor J_1' and J_2' between Er sublattices in the two-sublattice approximation. (b) The antisymmetric coupling constant between Er sublattices. (c) Effective g tensors of Er^{3+} ions.

(a)

	$\vec{\tilde{S}}_1$	$\vec{\tilde{S}}_2$
$\vec{\tilde{S}}_1$	$\begin{pmatrix}J'_{2xx} & J'_{2xy} & 0\\ J'_{2xy} & J'_{2yy} & 0\\ 0 & 0 & J'_{2zz}\end{pmatrix}$	$\begin{pmatrix}J'_{1xx} & 0 & 0\\ 0 & J'_{1yy} & 0\\ 0 & 0 & J_{1zz}\end{pmatrix}$
$\vec{\tilde{S}}_2$	$\begin{pmatrix}J'_{1xx} & 0 & 0\\ 0 & J'_{1yy} & 0\\ 0 & 0 & J'_{1zz}\end{pmatrix}$	$\begin{pmatrix}J'_{2xx} & J'_{2xy} & 0\\ -J'_{2xy} & J'_{2yy} & 0\\ 0 & 0 & J_{2zz}\end{pmatrix}$

(b)

$\vec{\tilde{S}}_1$	$(0\ \ 0\ \ D'_z)$

(c)

$\vec{\tilde{S}}_1$	$\begin{pmatrix}g_{xx} & g_{xy} & 0\\ g_{xy} & g_{yy} & 0\\ 0 & 0 & g_{zz}\end{pmatrix}$	$\begin{pmatrix}g_{xx} & -g_{xy} & 0\\ -g_{xy} & g_{yy} & 0\\ 0 & 0 & g_{zz}\end{pmatrix}$

$\langle\vec{S}\rangle$ and $\langle\vec{\tilde{S}}\rangle$, the well known formulas are obtained as follows:

$$|\langle\vec{S}_i\rangle|/S_0 = B_{3/2}(g\mu_B S_0 H_i^{Cr}/k_B T), \tag{6}$$

where

$$g\mu_B \vec{H}_i^{Cr} = -\frac{\partial\langle\mathcal{H}\rangle}{\partial\langle\vec{S}_i\rangle} \tag{7}$$

and

$$|\langle\vec{\tilde{S}}_k\rangle|/\tilde{S}_0 = B_{1/2}(\mu_B \tilde{S}_0 |\tilde{g}_k \vec{H}_k|^{Er}/k_B T), \tag{8}$$

where

$$\mu_B \tilde{g}_k' \cdot \vec{H}_k^{Er} = -\frac{\partial\langle\mathcal{H}\rangle}{\partial\langle\vec{\tilde{S}}_k\rangle}. \tag{9}$$

B_S is the Brillouin function of spin S, and H_i^{Cr} and H_k^{Er} are the effective field of Cr^{3+} and Er^{3+} ions in the sublattices i and k, respectively. S_0 represents the magnitude of the Cr^{3+} spin and $\tilde{S}_0$ for the Er^{3+} spin and k_B is the Boltzmann constant.

Equation (6) implies that the magnitude of the Cr^{3+} sublattice magnetization $|\langle\vec{S}\rangle|$ is a monotonically increasing function for temperatures below T_{N1}. Since we analyze the data only at sufficiently lower temperatures than T_{N1}, $|\langle\vec{S}\rangle|$ can be treated as independent of temperature and is given as S_0 in Sec. III B. However, the magnitude of the Er^{3+} sublattice magnetization $|\langle\vec{\tilde{S}}\rangle|$ depends on temperature and is an important parameter for treating the magnetic properties of $ErCrO_3$ at lower temperature.

B. Field-induced SR from Γ_1 to Γ_4

In this section, we investigate the observed abrupt spin reorientation from Γ_1 to Γ_4 under external magnetic field along the c axis. As shown in Fig. 8, we assume the Γ_{14} spin arrangement at first, calculate the free energy F_{14} in the Γ_{14} phase and find the stable spin arrangement by minimizing the free energy as follows:

$$\begin{aligned}&\langle S_{1x}\rangle = -\langle S_{2x}\rangle = S_0\cos\theta\cos\psi,\\ &\langle\tilde{S}_{1z}\rangle = \tilde{S},\end{aligned} \tag{10}$$

and

$$\langle\tilde{S}_{2z}\rangle = \tilde{S}\cos\Phi \quad (0 \le \Phi \le \pi), \text{ etc.}$$

where ψ, θ, and Φ are the canting angle of Cr^{3+} spins, the spin rotation angle of Cr^{3+} and Er^{3+} spins, respectively, as shown in Fig. 8. Then F_{14} at $T=0$ is given as

$$F_{14} = F_{14}^{Cr} + F_{14}^{Cr\text{-}Er} + F_{14}^{Er}, \tag{11}$$

where

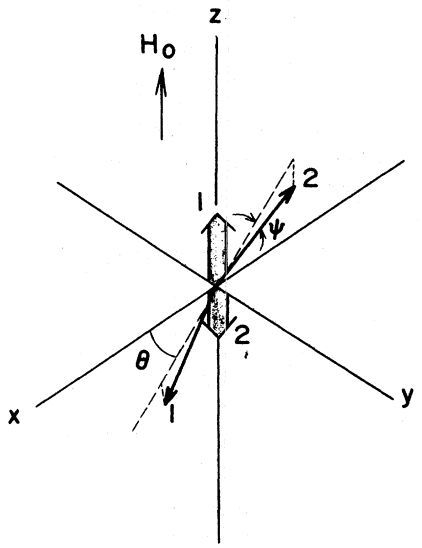

Γ_{14}

FIG. 8. Spin arrangement in the assumed Γ_{14} state. Long arrows represent Cr^{3+} spins and short arrows Er^{3+} spins. The external field is applied along the c axis. The state at $\theta=0$ corresponds to the Γ_4 phase and $\theta=\pi\frac{1}{2}$ to the Γ_1 phase.

$$\begin{aligned}F_{14}^{Cr} = &-JS_0^2\cos 2\psi - D_y S_0^2 \sin 2\psi\cos\theta\\ &-KS_0^2\cos^2\psi\cos^2\theta + g\mu_B S_0 \sin\psi H_0, \quad \text{etc.}\end{aligned} \tag{12}$$

From the conditions that minimize the free energy

$$\frac{\partial F_{14}}{\partial\psi} = \frac{\partial F_{14}}{\partial\theta} = \frac{\partial F_{14}}{\partial\Phi} = 0, \tag{13}$$

two stable spin arrangements are obtained as follows:

$$\begin{aligned}&\psi = (2D_y S_0 + 2\tilde{J}\tilde{S} - g\mu_B H_0)/4JS_0,\\ &\theta = \Phi = 0,\end{aligned} \tag{14}$$

which corresponds to the Γ_4 phase, and

$$\psi = -g\mu_B H_0/4JS_0, \quad \theta = \tfrac{1}{2}\pi, \quad \Phi = \pi, \tag{15}$$

which corresponds to the Γ_1 phase.

In these calculations, the order estimation of various exchange constants and that of the single ion anisotropy constants such as J, D_y, K, $\tilde{J}$, etc., by Yamaguchi was used and higher order terms were neglected (see Table II in Ref. 3).

Neglecting terms of higher order than ϵ^2, the free energy in the Γ_4 phase F_4 normalized by S_0^2, is

$$F_4 = -(J + D_y^2/2J + K) + 2(D_y'' + \tilde{a}_{zx})S + (J'_{1zz} + J'_{2zz} - \tilde{J}^2/2J)S^2 - g_{zz}\mu_B H_0 S/S_0 , \quad (16)$$

where

$$D_y'' = \tilde{D}_y - (\tilde{J}/2J)D_y , \quad (17)$$

$$S = |\langle \tilde{S} \rangle| / S_0 . \quad (18)$$

Similarly the normalized free energy F_1 in the Γ_1 phase is obtained as

$$F_1 = -J - 2(\tilde{D}_x - \tilde{a}_{yz})S - (J'_{1zz} - J'_{2zz})S^2 . \quad (19)$$

The ground state splittings of Er^{3+} are then calculated in our model, using Eqs. (7) and (9). The results are as follows: The ground-state splitting ΔE_4 in the Γ_4 phase is

$$\Delta E_4 = -2(D_y'' + \tilde{a}_{zx})S_0 - 2(J'_{1zz} + J'_{2zz} - \tilde{J}^2/2J)S_0 S + g_{zz}\mu_B(1 - \tilde{J}g/2Jg_{zz})H_0 , \quad (20)$$

and the ground-state splitting ΔE_1 in the Γ_1 phase is

$$\Delta E_1 = 2(\tilde{D}_x - \tilde{a}_{yz})S_0 - 2(J'_{1zz} - J'_{2zz})S_0 S . \quad (21)$$

Note that the ground-state splitting of Er^{3+} at $H_0 = 0$ has two contributions, the first one comes from the Cr^{3+}-Er^{3+} coupling and is independent of temperature at low temperature, while the second one comes from Er^{3+}-Er^{3+} couplings and depends upon temperature.

To calculate the free energy in each phase, we determine various exchange parameters and the single-ion anisotropy energy as follows. The Néel temperature T_{N1} is determined by the strongest exchange interaction J. In the simplest molecular-field approximation, J is given by

$$J = 3K_B T_{N1}/2S_0(S_0 + 1) . \quad (22)$$

For $ErCrO_3$, $T_{N1} = 133$ K and $S_0 = \frac{3}{2}$, then $J = 53.2$ K.

From the magnetization measurement[11] in $ErCrO_3$, $D_y = 3.72$ K and $K = 0.014$ K.

From the observed ground-state splittings ΔE_4 and ΔE_1, all other coefficients in the free energy in Eqs. (16) and (19) can be determined independently. Courths *et al.*[14] extensively measured ΔE_4 and ΔE_1 as functions of temperature and applied magnetic field. We also observed them and agree with their results. Therefore, we use their results below.

Then comparing the above results with the Eqs. (8), (18), (20), and (21), these coefficients are determined as follows:

$$\tilde{D}_x - \tilde{a}_{yz} = 3.28(\pm 0.05)\,\text{K},$$

$$D_y' + \tilde{a}_{zx} = -2.85(\pm 0.05)\,\text{K},$$

$$J'_{1zz} - J'_{2zz} = 3.62(\pm 0.34)\,\text{K},$$

$$\tilde{J}^2/2J - (J'_{1zz} + J'_{2zz}) = 3.57(\pm 0.33)\,\text{K},$$

and from their Zeeman measurement, $g_{zz} = 11.4(\pm 0.4)$, where $\tilde{J}g/2Jg_{zz}$ in Eq. (20) is negligible from the smallness of $\tilde{J}/J \sim \epsilon$.

Thus, as all the coefficients of the free energy are obtained, the magnetic field dependence of the free energies in the Γ_4 and Γ_1 phases can be calculated as shown in Fig. 9.

As shown clearly in Fig. 9, the field-induced SR from Γ_1 to Γ_4 occurs at $H_0 = H_c$. The calculated value of H_c is 0.87(±0.03) kOe. The agreement with the experiments is fairly good in spite of no adjustable parameters introduced in this calculation. The entropy term can be neglected at $T = 1.5$ K in comparing the free energies in each phase.

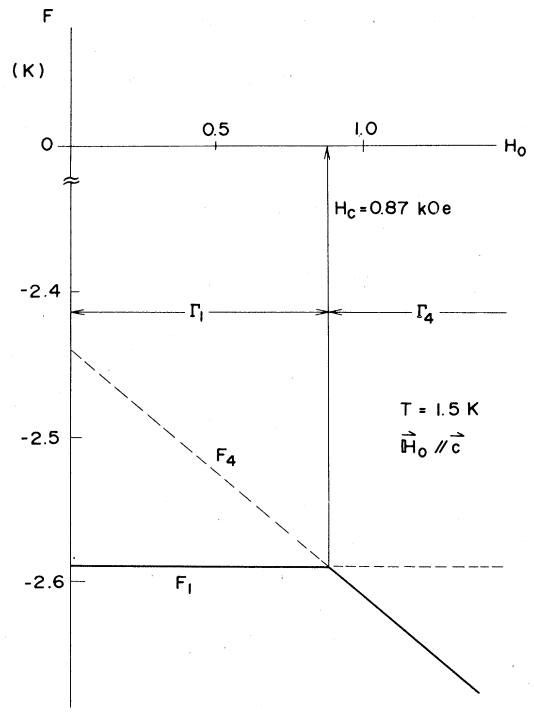

FIG. 9. Calculated free energy F_4 in Γ_4 (long-dash line) and F_1 in Γ_1 (short-dash line), using the formulas (18) and (21). The origin of the ordinate is set at $-J$. The field-induced SR fro . Γ_1 to Γ_4 occurs at $H_0 = H_c$. The solid line shows the energy of the stable states.

C. Field-induced SR from Γ_1 to Γ_2

The analysis of the Γ_2 phase is more difficult than that of the other phases, due to the large number of independent coupling coefficients allowed by symmetry in the Γ_2 phase. However, using the optical-spectroscopy data in the Γ_2 phase, most of the coefficients can be determined and the result of the field-induced SR from Γ_1 to Γ_2 can be explained quantitatively as follows. First, the free energy of the Γ_{12} phase under the external magnetic field is considered. With similar calculations to those of Sec. III B, two stable phases and spin arrangements, Γ_1 and Γ_2, are obtained. One is

$$\theta = 0, \tag{23}$$

$$\psi = (\tilde{J}S\sin\Phi - g\mu_B H_0/2S_0)/2J, \tag{24}$$

$$2(\tilde{D}_x - \tilde{a}_{yz})\tan\Phi + 2S[(J'_{1xx} + J'_{2xx}) + (J'_{1zz} - J'_{2zz}) - \tilde{J}^2/2J]\sin\Phi = \mu_B H_0(g_{xx} - \tilde{J}g/2J)/S_0, \tag{25}$$

which corresponds to the Γ_1 phase, and the other is

$$\theta = \tfrac{1}{2}\pi, \tag{26}$$

$$\psi = (D_y + \tilde{J}S\sin\Phi - g\mu_B H_0/2S_0)/2J, \tag{27}$$

$$2(\tilde{D}_x + \tilde{a}_{yz})\tan\phi + 2(D'_y - \tilde{a}_{zx}) + 2S \times[(J'_{1xx} + J'_{1yy}) + (J'_{2xx} - J'_{2yy}) - \tilde{J}^2/2J]\sin\Phi + 2S(J'_{2xy} + D'_z)\cos 2\Phi/\cos\Phi = \mu_B H_0(g_{xx} - \tilde{J}g/2J - g_{xy}\tan\Phi)/S_0, \tag{28}$$

which represents the Γ_2 phase.

Note that the canting angle of the Er spins, Φ, is a function of applied field H_0 along the a axis as shown in Eqs. (25) and (28). It is shown that Φ tends to zero when H_0 approaches zero in the Γ_1 phase. However, Φ does not tend to zero even when H_0 is zero in the Γ_2 phase, because in general the molecular field of the Er^{3+} spins in the phase is canted in the x-y plane.

Using the parameter Φ, the free energy and the ground-state splitting of the Er^{3+} ions in each phase can be simply described as follows.

In the Γ_1 phase, the ground-state splitting ΔE_1 is given as

$$\Delta E_1 = \frac{2(\tilde{D}_x - \tilde{a}_{yz})S_0 + 2(J'_{1zz} - J'_{2zz})S_0 S}{\cos\Phi}. \tag{29}$$

The normalized free energy F_1 is

$$F_1 = -J - 2(\tilde{D}_x - \tilde{a}_{yz})S\cos\phi - \tilde{J}^2S^2\sin^2\Phi/2J + S^2[(J'_{1xx} + J'_{2xx})\sin^2\Phi - (J'_{1zz} - J'_{2zz})\cos^2\Phi] - \mu_B H_0(g_{xx} - \tilde{J}g/2J)S\sin\Phi/S_0 - g^2\mu_B^2 H_0^2/8JS_0. \tag{30}$$

$$\Delta E_2 = [2(\tilde{D}_x + \tilde{a}_{yz})S_0 + 2(J'_{1yy} - J'_{2yy})S_0 S + \mu_B g_{xy}H_0]/\cos\Phi. \tag{31}$$

The normalized free energy F_2 is

$$F_2 = -(J + D_y^2/2J) + 2(D'_y - \tilde{a}_{zx})S\sin\Phi - 2(\tilde{D}_x + \tilde{a}_{yz})S\cos\Phi - \tilde{J}^2S^2\sin^2\Phi/2J + S^2[(J'_{1xx} + J'_{2xx})\sin^2\Phi - (J'_{1yy} - J'_{2yy})\cos^2\Phi + 2(J'_{xy} + D'_x)\sin\Phi\cos\Phi] - \mu_B H_0(g_{xx} - g\tilde{J}/2J)S\sin\Phi/S_0 - \mu_B H_0 g_{xy}S\cos\Phi/S_0 + (D_y/2J)g\mu_B H_0/S_0 - g^2\mu_B^2 H_0^2/8JS_0. \tag{32}$$

It should be remarked that there are several notable differences in the coefficients of ΔE_2 and F_2 in the Γ_2 phase from those in Γ_1 and Γ_4 phases. In the Cr-Er coupling coefficients, $\tilde{D}_x - \tilde{a}_{yz}$ in the Γ_1 phase and $D''_y + \tilde{a}_{zx}$ in Γ_4 convert to $\tilde{D}_x + \tilde{a}_{yz}$ and $D''_y - \tilde{a}_{zx}$ in the Γ_2 phase, respectively. These changes are important for the analysis as shown later. Secondly, for the Er-Er, coupling coefficients, the xx, yy, and xy components of the J'_1 and J'_2 tensors and the antisymmetric exchange term D'_z are involved in the Γ_2 phase, although, only the zz and xx components of J'_1 and J'_2 appear in Γ_1 and Γ_4 phases. The last notable points are related to the anisotropy of the g tensor of the Er ions. Not only the diagonal xx component but also the off-diagonal xy component of g, is involved in the Γ_2 phase with $\vec{H}_0 \| \vec{a}$.

The above coefficients are determined from the observed ground-state splittings of the Er^{3+} ions, in Fig. 4 as follows. It was shown that the data between $15.5 \leq T \leq 30$ K was nearly temperature independent and that at 4.2 K the splitting was slightly larger than the simple extrapolated values of these data at higher temperatures. We assume that the energy difference comes from the Er-Er coupling terms. So these data show that Er-Er coupling can be neglected for $T \geq 15$ K, and that this coupling gives a minor effect even at lower

temperatures in the Γ_2 phase.

We begin the analysis of data at higher temperatures without considering the Er-Er coupling terms. By putting the Er spin polarization parameter, S, to zero in Eqs. (28) and (31), one can calculate Φ and ΔE_2 in the Γ_2 phase as a function of H_0, where g_{xx} and g_{xy} are treated as adjustable parameters.

If one assumes that the $\tilde{a}$ term is negligible compared with the $\vec{\tilde{D}}$ term, and using the values $\tilde{D}_x = 3.28$ K, and $D_y = -3.62$ K, following the result in Sec. III B, the result drastically deviates from the experimental result. One example is shown by the dash-dotted curve in Fig. 4 with parameters $g_{xx} = 4.6$, $g_{xy} = 0$. The calculated results of ΔE_2 are always too large.

Therefore, this fact shows that the $\tilde{a}$ term cannot be neglected and that it reduces the ground-state splitting in the Γ_2 phase. Then we introduce a reduction factor and assume

$$\begin{aligned} \tilde{D}_x + \tilde{a}_{yz} &= \alpha(\tilde{D}_x - \tilde{a}_{yz}), \\ \tilde{D}_y - \tilde{a}_{zx} &= \alpha(D_y + a_{zx}), \end{aligned} \tag{33}$$

where α is treated as an adjustable parameter.

The best fitted result is shown by the dashed curve in Fig. 4 with

$$g_{xx} = 4.60, \quad g_{xy} = 0.0, \quad \alpha = 0.499.$$

The agreement is excellent. This result shows that the effective field at the Er spins induced by the $\vec{\tilde{a}}$ term, which has been neglected, is fairly large and is about 0.33 of the effective field due to $\vec{\tilde{D}}$ term in $ErCrO_3$. Both terms give rise to the effective fields which are orthogonal to those of the $\tilde{J}$ term and act as the driving force for the SR to occur.

Secondly, we analyze data at $T = 4.2$ K, taking into account the minor Er-Er coupling terms. We assume uniaxial anisotropy in the J_1' and J_2' tensors, i.e., $J'_{1xx} = J'_{1yy}$, $J'_{2xx} = J'_{2yy}$ and neglect the off diagonal component J'_{2xy} and the antisymmetric term D'_z for simplicity. We further assume that the J_1' and J_2' tensors are similar figures, i.e., $J'_{1xx}/J'_{1zz} = J'_{2xx}/J'_{2zz}$. Using the Eqs. (8), (9), (18), (28), and (31) and using parameters, formerly determined by experiments, one can calculate ΔE_2 and the best fitted result is shown by the solid curve in Fig. 4 with parameters as follows:

$$J'_{2zz} = -3.60 \text{ K}, \quad J'_{2xx}/J'_{2yy} = -0.23 \text{ K},$$
$$J_1' = 0, \quad \tilde{J}/J = 0.$$

Similar calculations with the determined parameters in the Γ_1 phase are performed and the result is shown by the dotted curve in Fig. 4. The agreement in lower fields is satisfactory, but not in higher fields. This result remains to be explained.

Finally, using the Eqs. (30) and (32), one can calculate the free energies F_1 and F_2 in the Γ_1 and Γ_2 phases as a function of H_0, respectively. One can also obtain the critical field H_c. The results are shown in Fig. 10. The solid curves are the ones at $T = 0$ K and the dashed curves are the ones at $T = 4.2$ K. The magnetic entropy differences can be neglected in this case because the Cr entropy is negligibly small at low temperatures and the Er entropy is a function of the ground-state splitting ΔE, which shows no discontinuity at the SR point from Γ_1 to Γ_2. The calculated H_c is 40 kOe at $T = 0$ K and 37 kOe at $T = 4.2$ K, which agrees excellently with the experimental results.

IV. CONCLUSIONS

The field-induced SR of $ErCrO_3$ has been observed by means of optical absorption of the Er^{3+} and Cr^{3+} ions. Under a field applied along the a axis at low temperature, SR from Γ_1 to Γ_2 is observed. No discontinuity of the ground-doublet splitting is observed with Er^{3+} ions. The observed critical field H_c is 37 kOe at $T = 1.5$ K. With the field along the c axis at low temperature, SR is observed from Γ_1 to Γ_4. The observed results are consistent with the other work.[6,14]

The observed nature of the field-induced SR in

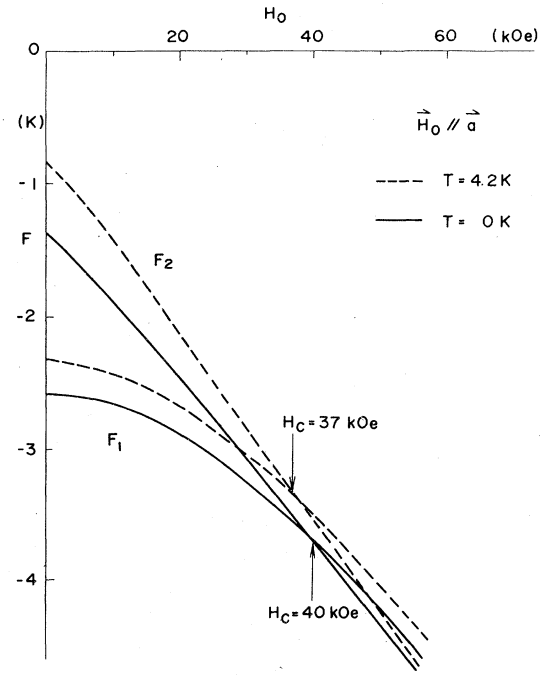

FIG. 10. Calculated free energies F_1 and F_2 in the Γ_1 and Γ_2 phases, respectively. Crossing of the F_1 and F_2 curves means that field-induced SR occurs.

$ErCrO_3$ can be understood quantitatively using the two-sublattice molecular-field model. It is shown for the first time that the anisotropic-symmetric-exchange interaction, $\vec{a}$ between Cr and the rare earth plays an important role in the SR mechanism along with the antisymmetric exchange interaction $\vec{D}$.

ACKNOWLEDGMENT

The authors sincerely thank Professor Sugano for stimulating discussions and Dr. Aoyagi and other staff members of the magneto-optics group at Nippon Hōsō Kyōkai where this work was carried out, for their useful advice and help in the experiments. They are grateful to Professor Kobayashi and Dr. Nakahara of the Institute for Solid State Physics, University of Tokyo, for permitting the use of and for helping with the high-field superconducting magnets. They are also indebted to Dr. Yamaguchi of Shizuoka University for enlightening discussions. Two of the authors (K.T. and S.K.) were partly supported by the Broadcasting Culture Fund.

---

*Present address: IBM Japan: Fujisawa-shi, Kanagawa-ken 252, Japan.

[1]K. Aoyagi, K. Tsushima, and S. Sugano, Solid State Commun. 7, 229 (1969).
[2]K. S. Meltzer, Phys. Rev. B 2, 2398 (1970).
[3]T. Yamaguchi, J. Phys. Chem. Solids 35, 479 (1974).
[4]T. Yamaguchi, S. Sugano, K. Tsushima, and S. Washimiya, *Proceedings of the International Conference of Magnetism ICM-73* (Nauka, Moscow, 1974), Vol. 5, p. 275.
[5]S. Sugano, K. Aoyagi, and K. Tsushima, J. Phys. Soc. Jpn. 31, 706 (1971).
[6]A. Hasson, R. M. Hornreich, Y. Komet, B. M. Wanklyn, and I. Yaeger, Phys. Rev. B 12, 5051 (1975).
[7]M. Kaneko, S. Kurita, and K. Tsushima, J. Phys. C 10, 1979 (1977).
[8]E. F. Bertaut and J. Mareschal, Solid State Commun. 5, 93 (1967).
[9]C. Veyret, J. B. Ayasse, J. Chaussy, J. Mareschal, and J. Sivardiere, J. Phys. (Paris) 31, 607 (1970).
[10]E. F. Bertaut, J. Mareschal, R. Pauthenet, and J. P. Rebouillet, Bull. Soc. Fr. Ceram. A75, 44 (1966).
[11]L. Holmes, M. Eibschütz, and L. G. Van Uitert, J. Appl. Phys. 41, 1184 (1970).
[12]M. Eibschütz, L. Holmes, J. P. Maita, and L. B. Van Uitert, Solid State Commun. 8, 1815 (1970).
[13]M. Eibschütz, R. L. Cohen, and K. W. West, Phys. Rev. 178, 572 (1969).
[14]R. Courths and S. Hüfner, Z. Phys. B22, 245 (1975).
[15]E. F. Bertaut, in *Magnetism III*, edited by G. T. Rado and H. Suhl (Academic, New York, 1963), p. 149.
[16]T. Yamaguchi and K. Tsushima, Phys. Rev. B 8, 5187 (1973).